METTL3 silencing suppresses cardiac fibrosis via m6A modification of SMOC2

Yanru He[1], Xiaodong Pan[1], Zaixiao Tao[2], Zhongpu Chen[1], genshan Ma[*,1], Sunkai Ling[*,3]

1. Department of Cardiology, Zhongda Hospital Affiliated to Southeast University, Nanjing, China
2. Department of Cardiology, School of Medicine, Southeast University, Nanjing, China
3. Department of Radiation Oncology, The First Affiliated Hospital of Nanjing Medical University, Nanjing, China

Corresponding author

Sunkai Ling, PhD, Department of Radiation Oncology, The First Affiliated Hospital of Nanjing Medical University, No.300 GuangZhou Road, Nanjing 210029, China.

Email: seulsk1031@163.com

Genshan Ma, MD, PhD, Department of Cardiology, Zhongda Hospital Affiliated to Southeast University, No. 87 DingJiaQiao Road, Nanjing 210009, China.

Email: magenshan@hotmail.com

1. Introduction

Heart failure (HF) is a significant public health issue affecting more than 23 million people worldwide[1]. With an aging population, its incidence has increased annually, imposing a huge medical burden on society[2, 3]. Among the numerous cardiovascular diseases, myocardial infarction (MI) is one of the main causes of HF. Necrotic myocardial cells are replaced by fibroblasts post-MI, forming fibrotic scars that prevent ventricular wall rupture following ischemic injury. Subsequently, owing to the increase in mechanical stress and activation of fibrogenic signalling pathways, fibroblasts in the infarct border zone further proliferate and differentiate, destroy the normal structure of myocardial tissue, reduce cardiac compliance, contribute to cardiac systolic and diastolic dysfunction, and ultimately lead to HF[3]. Therefore, clarifying the molecular mechanisms underlying the development of cardiac fibrosis post-MI can help identify new intervention targets for preventing, stabilizing, and even reversing HF and facilitate more precise clinical selection of anti-HF treatment strategies.

Our previous studies showed that epigenetic modifications participate in the proliferation and differentiation of cardiac fibroblasts (CFs)[4, 5]. m6A modifications are reportedly associated with the development of myocardial fibrosis. Inhibition of FTO, an m6A demethylase, attenuates the antifibrotic effect of leonurine in rat cardiac fibroblasts[6]. METTL3 catalyzes m6A methylation of GAS5 in a YTHDF2-dependent manner to boost mitochondrial fission and cardiac fibroblast proliferation and fibroblast migration[7]. Overexpression of methyltransferase METTL3 in CFs could upregulate the expression of fibrosis-related genes and activate the TGF- β/Smad2/3 signalling

pathway to promote the development of myocardial fibrosis[8]. METTL3 can also inhibit the expression of androgen receptors (AR) in an m6A-YTHDF2-dependent manner, thereby increasing cell glycolysis and promoting CF proliferation[9]. Despite these results, cardiac fibrosis remains a complex pathological process, necessitating further study of its specific molecular mechanisms to enhance the prognosis of heart failure.

SMOC2, a SPARC-related modular calcium-binding protein 2, is an encoded modular secretion protein that can affect the activity of cytokines, destroy the attachment of cell substrates, and regulate cell differentiation and cell cycle[10, 11]. SMOC2 is reportedly involved in the regulation of fibrotic diseases[12-14]. Moreover, SMOC2 suppression has been shown to alleviate myocardial fibrosis via the ILK/p38 pathway[15]. Several analyses of expression profile data have identified SMOC2's potential involvement in the pathogenesis of HF, indirectly suggesting its association with cardiac fibrosis[16, 17]. However, the question of whether METTL3 promotes cardiac fibrosis by affecting the methylation level of SMOC2 remains unclear. Consequently, we undertook this study to investigate the effect of METTL3 on cardiac fibrosis and to understand its specific mechanism.

2. Material and Methods

2.1 Animal care and treatments

Eight-week-old male C57BL/6 mice were purchased from Qing Longshan Animal Breeding Field (Nanjing, China). All animal experiments were approved by the Ethics

Review Board for Animal Studies of the Institute of Southeast University (Nanjing, China) and adhered to the established guidelines published by the US National Institutes of Health. Under standard environmental conditions, all animals were housed and had ad libitum access to food and water.

The mice were randomly divided into sham, 7dpmi (7-day post-MI), 14dpmi (14-day post-MI) and 28dpmi (28-day post-MI) groups (n = 6 per group) and underwent surgical induction of MI by permanent coronary ligation or sham operation. Briefly, the mice were anesthetized intraperitoneally with sodium pentobarbital (50 mg/kg, Merck, Germany). Following endotracheal intubation, they were placed on a ventilator, and a left lateral thoracotomy was performed to expose the left ventricle. The left coronary artery was ligated using an 8−0 silk suture. Successful ligation was confirmed by observing left ventricular pallor immediately after ligation. Mice in the sham group underwent similar surgery without ligation.

To investigate the role of METTL3 in vivo, AAV9 carrying a periostin promoter driving the expression of short hairpin RNA (shRNA) targeting METTL3 (AAV9-periostin promoter-eGFR-shMETTL3, AAV9-shMETTL3, TAATGTCCCATACGGTAGCTC) or a negative control (AAV9-periostin promoter-eGFR-shNC, AAV9-shNC, ACGTGACACGTTCGGAGAA) was constructed by Shanghai GeneChem Co. (Shanghai, China). Briefly, the mice were randomly divided into four groups: AAV9-shNC + sham (n = 6), AAV9-shNC +MI (n =6), AAV9-shMETTL3 +sham (n =6), and AAV9-shMETTL3+MI. At 3 days post MI or sham operation, each mouse was injected with AAV9-shMETTL3 or AAV9-shNC containing 2.5×10^{11} viral genome particles via

the tail vein.

At 4 weeks post-treatment, the animals were sacrificed after excessive inhalation of CO_2 and their hearts were harvested.

2.2 Cell culture and treatment

CFs were isolated from freshly euthanized C57BL/6 mice through enzymatic digestion, following a standard protocol[18]. Briefly, mouse hearts were rapidly excised, minced, and placed in cold phosphate buffered saline (PBS). The minced tissue was subsequently digested with a collagenase II (#V900892, Sigma-Aldrich, MO)/trypsin (Solarbio Life Sciences, Beijing) solution at 37℃ for 8 min. After six to seven digestion periods, the supernatants were centrifuged to collect the cells. Cells were resuspended in DMEM/F12 (#11320033, Gibco, MA) and incubated for 90 min to allow CFs to attach to the dishes. Subsequently, the cells in the medium were discarded. CFs were incubated at 37℃ in a humidified atmosphere of 5% CO_2 and grown to 70–80% confluence. CFs were further cultured and passaged at a 1:3 dilution. Second- to fourth-passage CFs were used in the experiment.

2.3 Dot blot assay

RNA samples were isolated and purified using TRIzol reagent according to the standard protocol. After quantification and denaturation (95℃, 5 min), mRNA was loaded onto Amersham HyBond N+ membranes (Amersham, UK). Subsequently, the membrane was crosslinked with UV light for 5 min, followed by staining with 0.02% Methylene blue. Photographs were taken to determine the input RNA content. Subsequently, the membranes were washed with PBST and then blocked with 5%

defatted milk for 1 h, followed by incubation with an m6A antibody (1:1000; Epigentek, #A-1801) at 4℃ overnight. Dotted blots were visualized after incubation with secondary antibodies.

2.4 m6A RNA methylation quantification

An EpiQuik m6A RNA methylation quantification kit (Epigentek Group Inc., Farmingdale, NY, USA, P-9005) was used to quantify N6-methyladenosine RNA methylation. Briefly, 300 ng of RNA was added to the wells, followed by the addition of capture antibody solution. Then, the detection antibody solution was added to the assay wells according to the manufacturer's protocol. The m6A levels were quantified using colorimetry by reading the absorbance of each well at 450 nm.

2.5 Histology

The hearts were perfused with ice-cold PBS to eliminate blood contamination and fixed in 4% paraformaldehyde overnight. Subsequently, they were embedded in paraffin and cut into sections of 5-μm thickness. Masson's trichrome staining was performed according to standard methods.

2.6 MeRIP-qPCR

The m6A immunoprecipitation (MeRIP) procedure was performed using the MeRIP™ m6A kit (17-10499, Magna) according to the manufacturer's published instructions. Briefly, mRNA was fragmented and immunoprecipitated with Protein A beads pre-incubated with the anti-m6A antibody (ab208577, Abcam) in IP buffer. After elution, qPCR was performed to determine the mRNA levels. MeRIP-qPCR was performed in triplicates. The primer sequences used are listed as Table 1.

2.7 Western blot analysis

Proteins were extracted using a Protein Extraction kit (KeyGEN Biotech, #KGB5303-100), and their concentrations were determined using the BCA Protein Assay Kit (KeyGEN Biotech, #KGB2101-1000). Subsequently, the proteins were separated by SDS-PAGE and transferred onto PVDF membranes, which were then blocked with TBST containing 5% skimmed milk powder. Following blocking, the membranes were incubated overnight at 4℃ with specific primary antibodies and subsequently detected using an ECL protocol with horseradish peroxidase-conjugated IgG as the secondary antibody. Primary antibodies were utilized according to the manufacturer's instructions (Table 2).

2.8 Echocardiography

Echocardiography was performed using a Visual Sonics Vevo3100 small-animal ultrasound scanner (FUJIFILM Visual Sonics, Inc) to assess cardiac function. Mice were anesthetized with 1.5% isoflurane and put in a supine position. Data from three consecutive cardiac cycles were analyzed for each measurement. Left ventricular systolic dimension (LVDs), left ventricular diastolic dimension (LVDd), and the thickness of the septal and posterior wall thicknesses were measured. LV systolic volume (LV Vol s), LV diastolic volume (LV Vol d), LV ejection fraction (LVEF), and fractional shortening (FS) were calculated from these measurements.

2.9 Cell transfection

Specific shRNAs against METTL3/SMOC2 and control shRNAs were synthesized by Shanghai GeneChem Co. (Shanghai, China). CFs were transfected with either

shMETTL3/shSMOC2 or shRNA using Lipofectamine 3000 transfection reagent (Invitrogen, Carlsbad, USA). Relative shRNA sequences were as Table 3.

2.10 Cell counting kit-8 assay

CFs were inoculated in 96 well plates and transfected with shNC or shMETTL3 under normoxic or hypoxic conditions for 48 h. Thereafter, 10 μL of CCK-8 solution was added to each well and incubated for 2 h. The absorbance of each well was measured at 450 nm using a microplate reader (ELx800, Bio-tech, Germany). Viability = (absorbance of sample)/ (absorbance of control).

2.11 5-Ethynyl-2′-deoxyuridine (EdU) incorporation assay

The EdU assay was procured from Donghuan (Shanghai, China). Initially, cells were treated with shNC, shMETTL3, or shSMOC2 under normoxic or hypoxic conditions for 48 h. Subsequently, the cells were incubated with 10 μM EdU solution for an additional 2 h. After fixation with 4% formaldehyde and the addition of 150 μL glycine, the cells were incubated with 0.5% Triton X-100. Apollo reaction reagent (1×) was introduced, and then the cells were stained with 300 μL Hoechst (5 μg/mL) in darkness. EdU-labeled and unlabeled cells were then counted under a microscope (TE2000-U; Nikon), and pictures were taken.

2.12 Immunofluorescence of tissue sections

Paraffin-embedded heart tissue sections were rehydrated in a series of graded ethanol solutions, followed by heating in ethylenediaminetetraacetic acid (EDTA) antigen retrieval buffer (ShareBio, SB-MY001) at a low boiling point for 15 min. Subsequently, the sections were blocked with 1 % BSA for 1 h. Primary antibodies against METTL3

and SMOC2 were incubated overnight, followed by a 2-h incubation with secondary antibodies. Nuclear staining was performed using DAPI stain. Images were captured using a Picture Scanner (Pannoramic MIDI, 3DHISTECH, Hungary) and analyzed by Image Auto Analysis System (C.V.2.4, Servicebio, China).

2.13 Bioinformatic analysis

2.13.1 scRNA-seq analysis

The scRNA-seq dataset GSE145154 of MI was retrieved from the GEO database (https://www.ncbi.nlm.nih.gov/), comprising scRNA-seq data from left ventricle tissues of three infarcted myocardium and one healthy person. Large gene expression matrices were created using the “merge” function. Cells with >500 genes, <5,000 genes and <20% mitochondrial genes were retained. Gene expression lists were normalized using the “Normalize Data” function and further scaled. The samples were integrated using the anchors method in the R package "Seurat", and core cells were obtained by filtering scRNA-seq. Principal component analysis (PCA) was performed on single-cell samples, and 20 PCs were selected for UMAP algorithm analysis. Using the R package "Harmony,” 10 cell clusters were classified using the “FindClusters” function, and each cluster was manually annotated by the CellMarker database. Differential analysis was performed by using the “limma” package. P-value <0.05 and |Log2FC| >1 was designated as differentially expressed genes (DEGs). The "ggplot2" package was used to show the localization of genes.

2.13.2 MeRIP-seq analysis

The MeRIP-seq dataset GSE131296 of MI was retrieved from the GEO database

(https://www.ncbi.nlm.nih.gov/) and contained four ischemic group samples and 10 normal group samples. The R package “DESeq2” was used for differential analysis; P-value < 0.05 and |Log2FC|> 1 were designated as DEGs. The “pheatmap” package was used to depict the top DEGs. Then, GO and KEGG enrichment analyses were performed using the “clusterprofile” function.

2.13.3 Protein-ligand interaction analysis

Obtain the METTL3 protein structure from the Uniprot database and model SMOC2 mRNA using the Build and Edit Hucleic Acid module in Discovery Studio 2019 Client software. Conduct protein-nucleic acid docking through HDOCK server. Use the PLIP interaction analysis platform to comprehensively describe and systematically analyze the binding sites.

2.14 mRNA stability analysis

Following transfection, CFs were incubated with actinomycin D (2 mg/mL; Sigma-Aldrich) for 0, 3, and 6 h, and SMOC2 expression was examined using RT-qPCR.

2.15 Statistical analyses

Quantitative data were expressed as the mean ± standard deviation. All data were analyzed using IBM SPSS Statistics for Windows version 26.0 (IBM Corp., Armonk, N.Y., USA). Student’s t-test was employed to determine the statistical significance between the two groups, while one-way analysis of variance (ANOVA) was used for comparisons of data among multiple groups. Bioinformatic analyses were conducted using R language (Version 4.0.3). A significance level of $p< 0.05$ was regarded as a statistically significant difference, while $p < 0.01$ indicated a high statistically significant

difference.

3. Results

3.1 Increased m6A and METTL3 in fibrotic tissue of mice and Hypoxia-treated CFs.

A cardiac fibrosis mouse model was established by ligating the left anterior descending coronary artery for 4 weeks. Masson's trichrome staining revealed an increase in cardiac collagen deposition (Fig. 1A) accompanied by a deterioration in LVEF and FS post-MI (Fig. 1B). Furthermore, we quantified m6A levels in RNA extracted from fibrotic tissues and hypoxia-treated CFs, comparing them with m6A levels in sham surgical controls and normoxia-treated CFs. The increase in m6A in total RNA was observed as early as 7 days post-MI in mice (Fig. 1C). We also observed a sustained increase in the m6A levels after 24, 48, and 72 h of hypoxia (Figs. 1D & E). To identify the regulators of elevated m6A levels in fibrotic tissues and hypoxia-treated CFs, we measured the expression of several known proteins associated with m6A methylation. Western blotting demonstrated that the protein expression level of METTL3 was significantly increased in fibrotic tissues and hypoxia-treated CFs (Figs. 1F and G). Collectively, these data establish that METTL3 could be an important molecular hallmark that may regulate myocardial fibrosis post-MI by increasing m6A methylation.

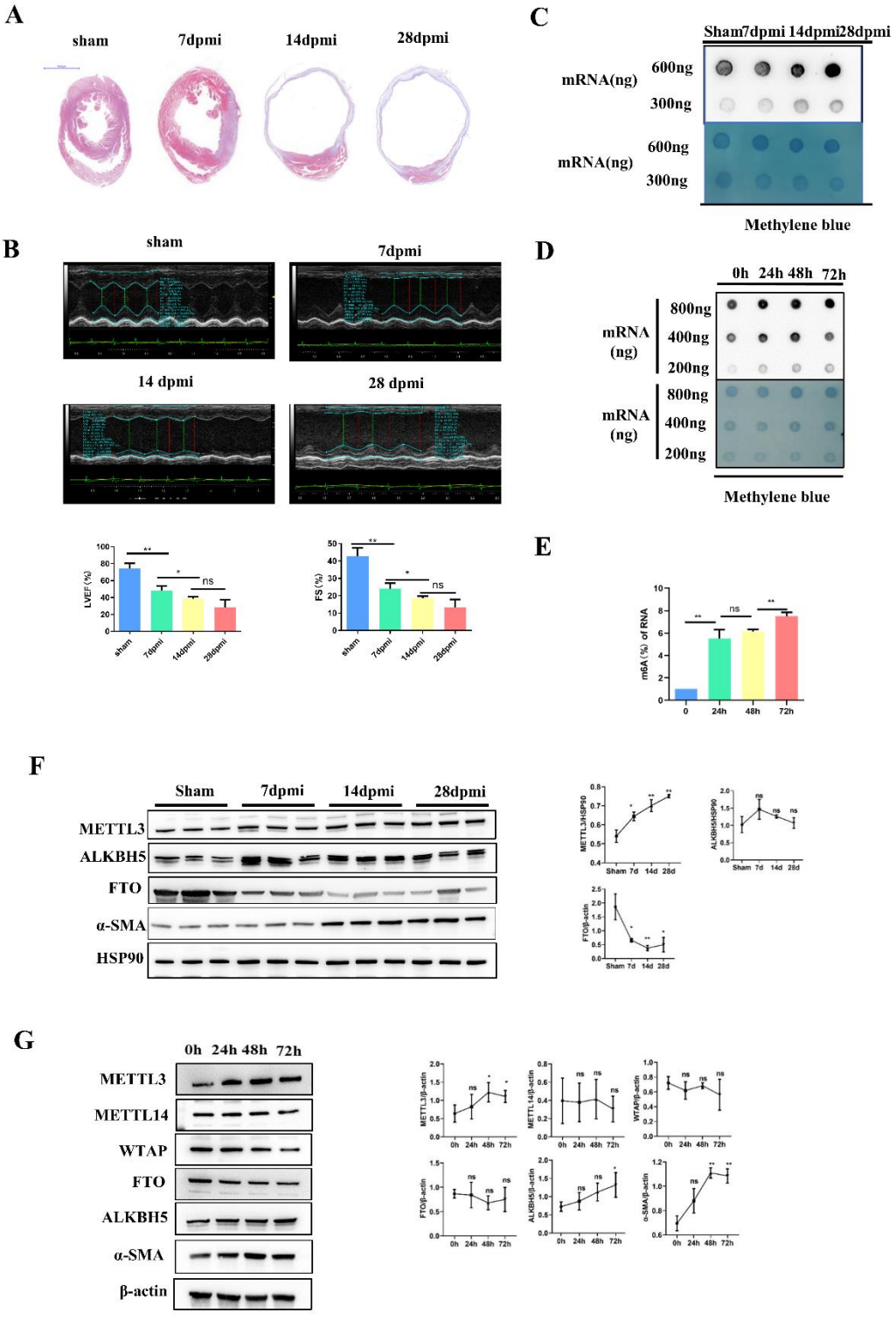

Fig. 1: Increased m6A and METTL3 in fibrotic tissue of mice and Hypoxia-treated CFs. A) Masson staining was used to analyze the degree of collagen deposition in the cardiac tissue of sham, 7dpmi, 14dpmi and 28dpmi groups; B) Echocardiography was

used to analyze of left ventricular ejection fraction and fractional shortening of sham, 7dpmi, 14dpmi and 28 dpmi groups; C) Dot blot was used to detect the level of m6A of mRNA in left ventricular tissue of sham, 7dpmi, 14dpmi and 28dpmi groups; D&E) Dot blot and m6A RNA methylation quantification were used to detect the levels of m6A of mRNA in CFs under hypoxia conditions at 0, 24, 48 and 72 h; F) Western blot was used to analyze the expression of METTL3, ALKBH5, FTO, α-SMA, HSP90 in left ventricular tissue of sham, 7dpmi, 14dpmi and 28dpmi groups; G) Western blot was used to analyze the expression of METTL3, METTL14, WTAP, ALKBH5, FTO, α- SMA, β-actin in CFs under hypoxia conditions at 0, 24, 48 and 72 h. * Indicating significant statistical differences: * $p<0.05$ and * * $p<0.01$. Sham: sham surgery group; 7dpmi: 7 days after myocardial infarction; 14dpmi: 14 days after myocardial infarction; 28dpmi: 28 days after myocardial infarction; LVEF: left ventricular ejection fraction; FS: fractional shortening.

3.2 METTL3-mediated m6A modification regulates the proliferation and differentiation process of cardiac fibroblasts and the progression of cardiac fibrosis post-MI.

To investigate whether METTL3 regulates the proliferation and differentiation of cardiac fibroblasts (CFs), we constructed sh-METTL3 to knockdown METTL3 expression (Fig. 2A). CFs were treated with hypoxia and transfected with sh-METTL3 for 48 h. We found that METTL3 downregulation significantly abrogated the hypoxia-induced increase in α-SMA expression (Fig. 2B). Meanwhile, by using CCK-8 assay, we found that downregulation of METTL3 significantly abrogated the hypoxia-induced

proliferation (Fig. 2C). The EdU incorporation assay results were consistent with the CCK-8 assay (Fig. 2D). In vivo, we constructed AAV9-periostin promote-eGFP-shMETTL3 (AAV9-shMETTL3), which specifically knocked down METTL3 in fibroblasts (Fig. 2E). Three days post-MI, AAV9-shMETTL3 was injected into the tail vein of mice (Fig. 2E). Four weeks after the operation, AAV9-shMETTL3 directionally knocked down the expression of METTL3 in the ischemic myocardium group without affecting the normal group. We also found that the expression of α-SMA was decreased upon knockdown of METTL3 (Fig. 2F). Moreover, the collagen deposition area was reduced (Fig. 2G), and heart function was improved (Fig. 2H) in the MI+AAV9-shMETTL3 group compared to the MI +AAV9-sh-NC group. These results indicated that METTL3 regulates the proliferation and differentiation of CFs and the progression of cardiac fibrosis post-MI.

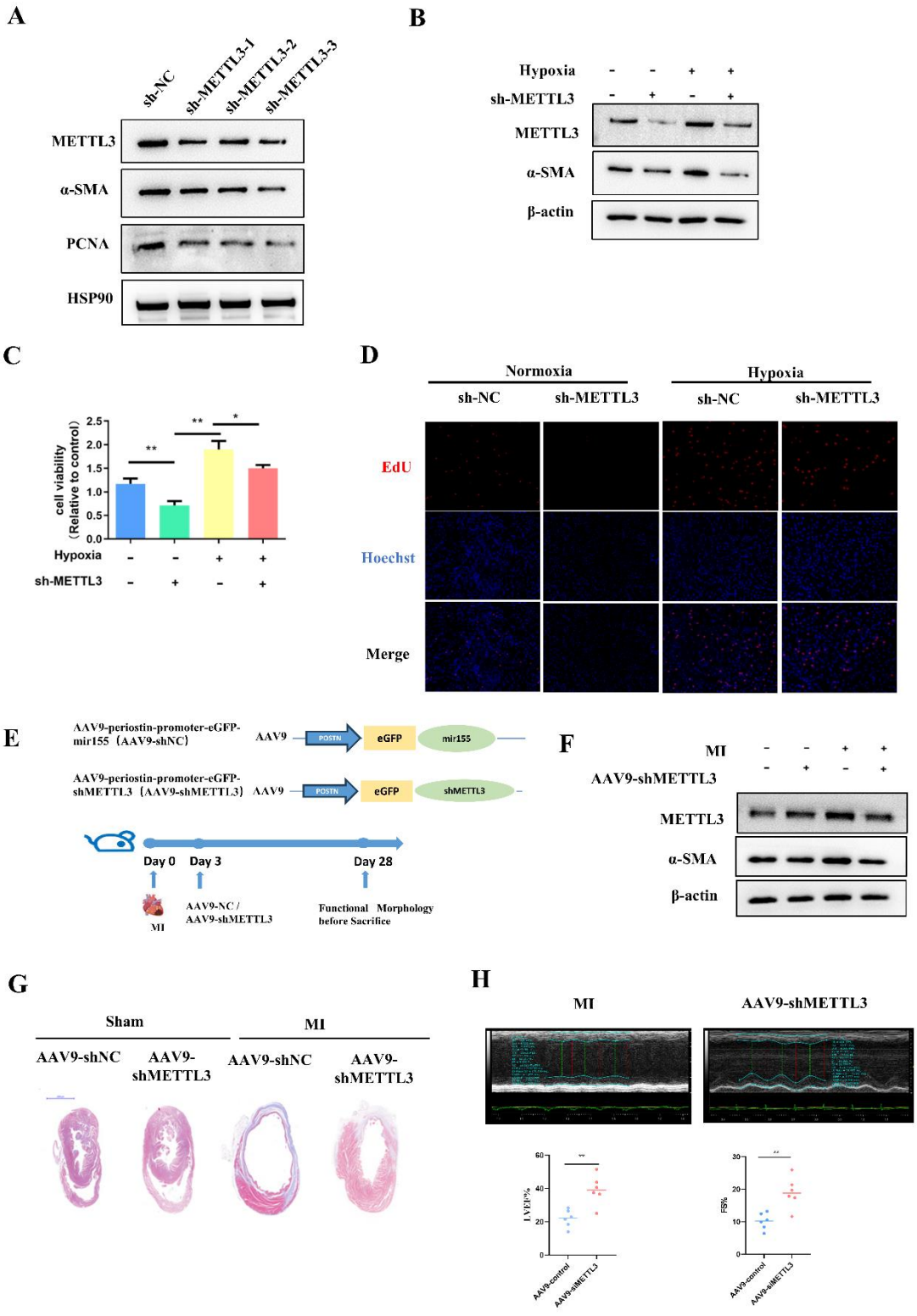

Fig. 2: METTL3-mediated m6A modification regulates the proliferation and differentiation process of cardiac fibroblasts and the progression of cardiac fibrosis post-MI. A) Western blot was used to analyze the expression of METTL3, α-

SMA, PCNA and HSP90 in CFs with the treatment of sh-NC or sh-METTL3; B) Western blot was used to analyze the expression of METTL3, α-SMA and HSP90 in CFs after treating with shNC or shMETTL3 under normoxic or hypoxic conditions; C&D) CCK-8 and EdU assay were used to detect the proliferation degree of CFs after treating with shNC or shMETTL3 under normoxic or hypoxic conditions; E) Construct AAV9-periostin promoter-eGFR-shMETTL3 and AAV9-periostin promoter-eGFR-shNC, each mouse was injected with AAV9-shMETTL3 or AAV9-shNC via tail vein at 3 days post MI or sham operation; F) Western blot was used to analyze the expression of METTL3, α-SMA and β-actin in left ventricular tissue with the treatment of AAV9-METTL3 or AAV9-shNC under MI or sham operation; G) Masson staining was used to analyze the degree of collagen deposition in left ventricular tissue with the treatment of AAV9-METTL3 or AAV9-shNC under MI or sham operation; H) Echocardiography was used to analyze of LVEF% and FS% in mice with the treatment of AAV9-METTL3 or AAV9-shNC under MI or sham operation; * Indicating significant statistical differences: * $p<0.05$ and * * $p<0.01$; LVEF: left ventricular ejection fraction; FS: fractional shortening

3.3 SMOC2 may be a key gene regulated by RNA methylation during the proliferation and differentiation of cardiac fibroblasts.

To further reveal the mechanism of CFs proliferation and differentiation after myocardial infarction, we utilized the GEO database (https://www.ncbi.nlm.nih.gov/geo/) to retrieve the single-cell RNA Sequencing (scRNA-Seq) dataset GSE145154 and the Methylated RNA Immunoprecision Sequencing (MeRIP-Seq) dataset GSE131296. Thereafter, we performed a secondary

analysis on the gene expression profiles of normal humans and patients with ischemic cardiomyopathy heart tissues. We then used Log FC>1 and $p<0.05$ as the screening conditions to obtain differential genes (Figs. 3A & B). Thirty-four differentially expressed genes (DEGs) were identified when we combined the two aforementioned differential genomes (Fig. 3C). Subsequently, we conducted GO and KEGG analyses using these 34 differential genes to further investigate their potential functions and affected pathways (Fig. 3D). Further analysis showed that SMOC2, one of the 34 differentially expressed genes, possessed multiple highly confident m6A methylation sites (Fig. 3E) and exhibited relatively high expression abundance in the FB cluster (Fig. 3F).

To further clarify the role of SMOC2 in the proliferation and differentiation of CFs, we used western blotting to detect the expression levels of SMOC2 in mouse myocardial fibrosis tissues and hypoxic intervention in CFs after MI. Results showed that the expression level of SMOC2 gradually increased with prolonged ischemia and hypoxia time in myocardial fibrosis tissues and hypoxic intervention in CFs after MI (Figs. 3G & H). Knockdown of SMOC2 in CFs did not affect the expression of METTL3 but regulated the proliferation and differentiation of CFs (Figs. 4A & B). However, regulating the expression of METTL3 in a myocardial fibrosis model after MI or hypoxia intervention in CFs can affect the expression level of SMOC2 (Figs. 4C &D); therefore, we initially believe that METTL3 can affect the proliferation and differentiation of CFs by regulating the expression level of SMOC2.

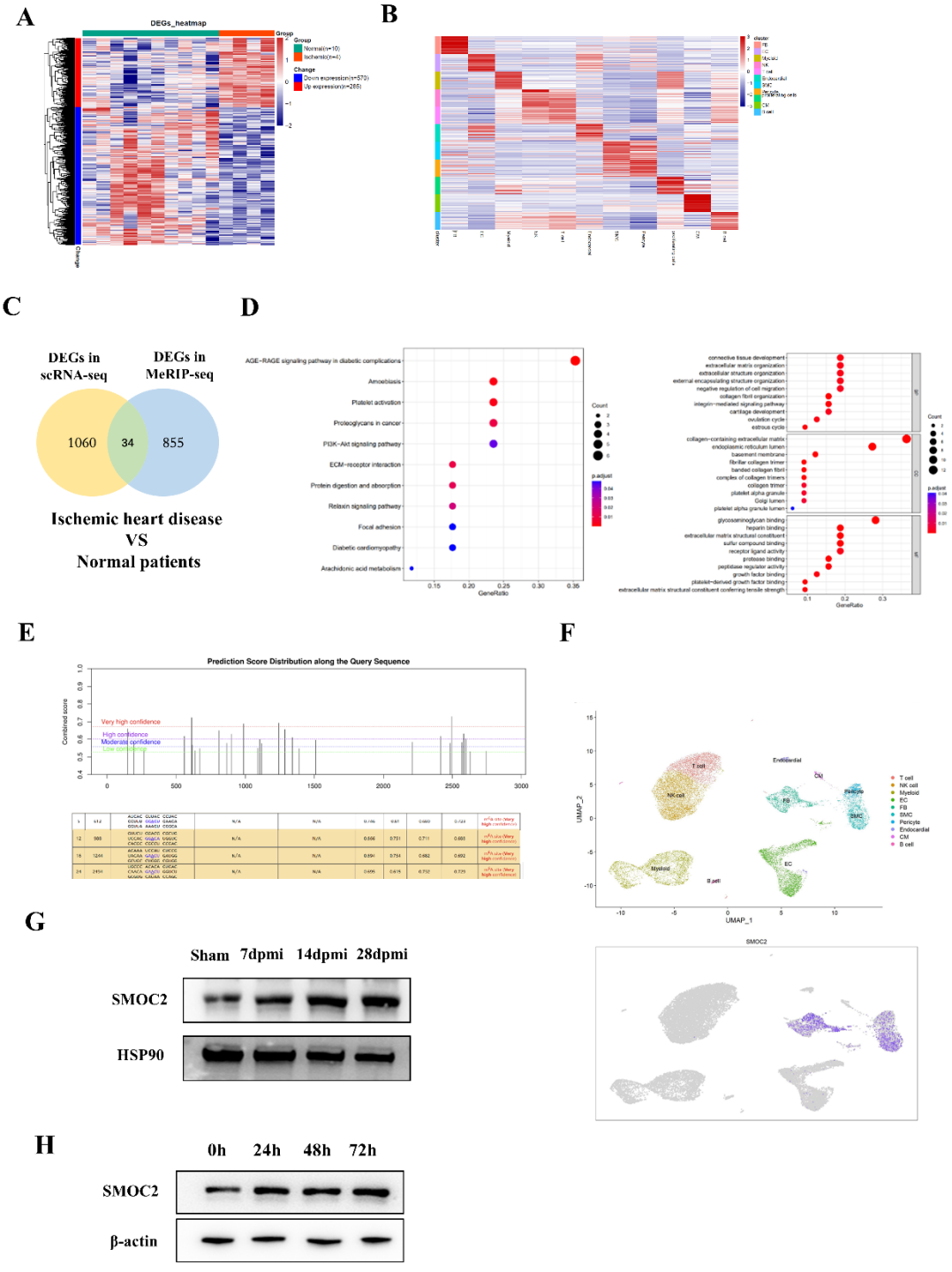

Fig. 3: SMOC2 may be a key gene regulated by RNA methylation during the proliferation and differentiation of cardiac fibroblasts. A) Comparison of differentially expressed genes in myocardial tissue RNA methylation sequencing results between patients with ischemic cardiomyopathy and normal individuals through

heatmap analysis; B) Cluster analysis of single-cell sequencing results of myocardial tissue from patients with ischemic cardiomyopathy and normal individuals using UMP; C) The Venn diagram displays the same differentially expressed genes in RNA methylation sequencing and single-cell sequencing of myocardial tissue between patients with ischemic cardiomyopathy and normal individuals; D) KEGG analysis reveals the signaling pathways that differentially expressed genes may participate in; GO analysis showcases the potential functions of differentially expressed genes; E) The methylation sites of METTL3 on SMOC2 were predicted using the SRAMP database; F) Single-cell sequencing showcases the expression of SMOC2 in fibroblast clusters; G) Western blot was used to analyze the expression of SMOC2 and HSP90 in left ventricular tissue of sham, 7dpmi, 14dpmi and 28dpmi groups; H) Western blot was used to analyze the expression of SMOC2 and β-actin in CFs under hypoxia conditions at 0, 24, 48 and 72 h; Sham: sham surgery group; 7dpmi: 7 days after myocardial infarction; 14dpmi: 14 days after myocardial infarction; 28dpmi: 28 days after myocardial infarction.

3.4 METTL3 regulates SMOC2 expression by increasing the stability of SMOC2 mRNA.

To elucidate the mechanism by which METTL3 regulates SMOC2 expression, we examined the effects of METTL3 on SMOC2 methylation. As shown in Fig. 3E, multiple methylation sites were predicted. Among these, four sequences were the most likely binding sites (Fig. 3E). PLIP was used to analyze the interaction core sites between METTL3 and SMOC2 mRNA. As the result shown in Fig.4E, binding sites exist

between the METTL3 and SMOC2 mRNA. We conducted MeRIP-qPCR experiments and found that METTL3 affected the binding of m6A to SMOC2 mRNA (Fig. 4F). Actinomycin D experiments showed that the METTL3 knockdown reduced the stability of SMOC2 mRNA (Fig. 4G). Therefore, we considered that METTL3 regulated the expression of SMOC2 by affecting the stability of SMOC2 mRNA, thereby affecting the proliferation and differentiation of cardiac fibroblasts.

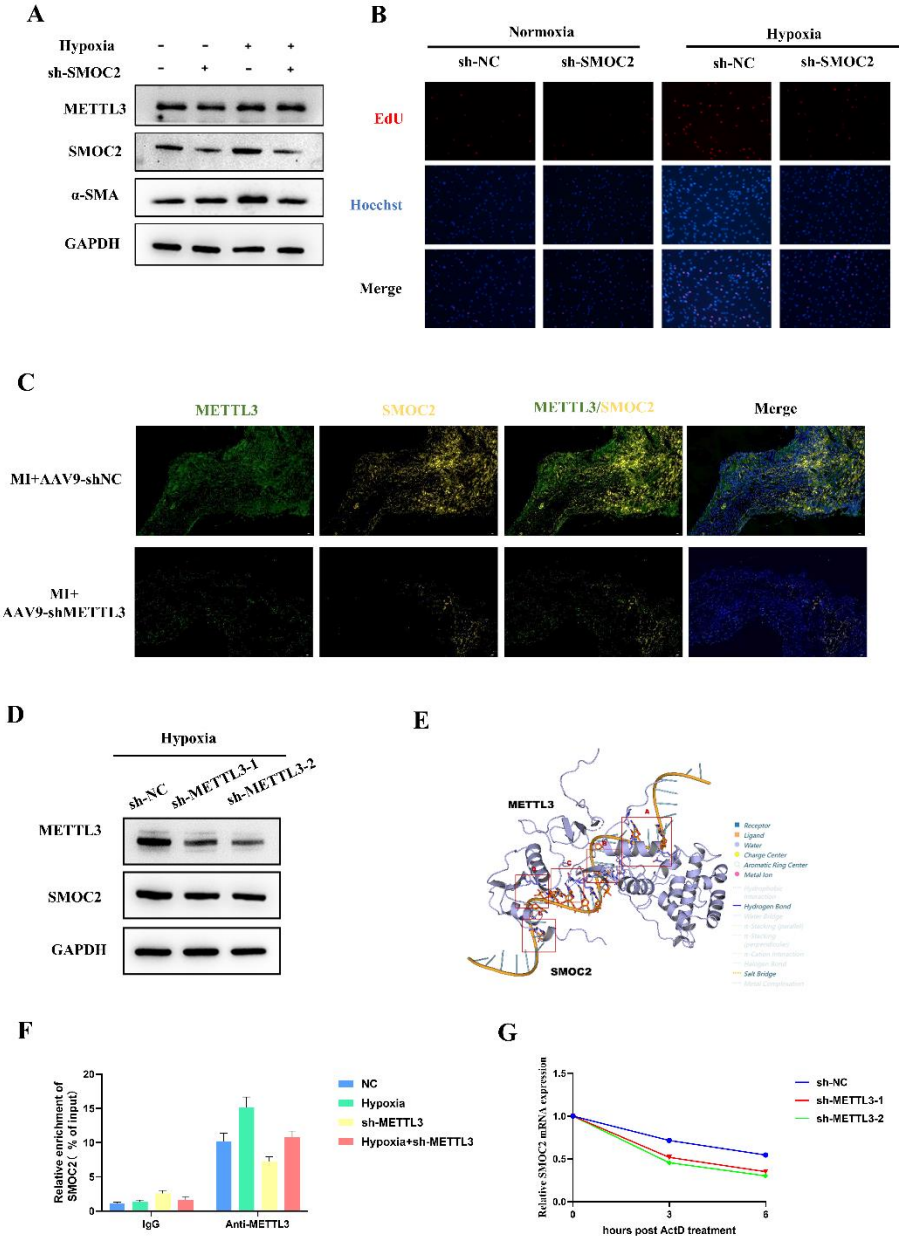

Fig. 4: METTL3 regulates SMOC2 expression by increasing the stability of SMOC2 mRNA. A) Western blot was used to analyze the expression of METTL3, SMOC2, α-SMA and GAPDH in CFs after treating with shNC or shSMOC2 under normoxic or hypoxic conditions; B) EdU assay was used to detect the proliferation degree of CFs after treating with shNC or shSMOC2 under normoxic or hypoxic conditions. C) Immunofluorescence was used to detect the expression of METTL3 and SMOC2 in left ventricular tissue with the treatment of AAV9-METTL3 or AAV9-shNC under MI operation; D) Western blot was used to analyze the expression of METTL3, SMOC2, α-SMA and GAPDH in CFs with the treatment of shNC, shMETTL3-1 or shMETTL3-2 under hypoxic conditions; E) The interaction core sites of METTL3 and SMOC2 were predicted using the PLIP; F) MeRIP-qPCR was used to detect the SMOC2 mRNA expression in CFs with the treatment of shMETTL3 or shNC under normoxic or hypoxic condition; G) The stability of SMOC2 was evaluated using RT-qPCR after actinomycin D treatment.

4. Discussion

M6A methylation modification may be a potential target for the treatment of heart failure[19, 20]. The proliferation and differentiation of cardiac fibroblasts are key pathological processes in the progression of heart failure[21-23]. Studies have indicated the involvement of m6A methylation modification in the proliferation and differentiation of cardiac fibroblasts[24-26], a finding corroborated by our study, which observed increased m6A methylation in a model of hypoxia-induced cardiac fibroblast proliferation and differentiation, as well as cardiac fibrosis post-MI. Moreover, the level

of m6A methylation increased with the extension of hypoxia and ischemia time. Three types of molecules are implicated in the modification of m6A: the m6A methyltransferase complex (METTL3, METTL14, and WTAP complex), RNA demethylase FTO and ALKBH5, and binding proteins containing the YTH domain[27, 28]. However, controversy persists regarding the enzymes that play major roles in the proliferation and differentiation of cardiac. METTL3[7, 9, 29], WTAP[30] and FTO[6] reportedly regulate CF proliferation and differentiation. Our study found that in cardiac fibrotic tissue post-MI, the expression of METTL3 and ALKBH5 increased, whereas that of FTO decreased with the extension of ischemia time. However, in CFs treated with hypoxia, the expression of METTL3 and ALKBH5 was upregulated with the extension of hypoxia time, whereas the expression of FTO and other m6A relative enzymes was not significantly different. Meanwhile, the knockdown of METTL3 in vivo and in vitro can reduce the expression of α-SMA, inhibit the proliferation of CFs, reduce the area of cardiac fibrosis post-MI and improve cardiac function. Combined with the results showing that m6A methylation was increased in CFs treated with hypoxia and in cardiac fibrotic tissue post-MI, we believe that METTL3 plays a key role in regulating the proliferation and differentiation of CFs via m6A methylation.

METTL3 mainly regulates the expression of target genes by affecting m6A methylation levels through post-transcriptional modification[24]. METTL3 also regulates m6A levels and the expression of collagen-related genes [8], IGFBP3 [31], androgen receptors[9], and lncRNA GAS5, all of which affect the proliferation and differentiation of CFs. With advances in next-generation sequencing technology, an increasing number of genes

have been thoroughly explored. In this study, we conducted a secondary analysis of scRNA-seq and MeRIP-seq data from myocardial ischemic tissue samples obtained from the GEO database. Through this analysis, we identified 34 DEGs regulated by m6A and associated with myocardial fibrosis. Among these, the role of SMOC2 piqued our interest. As previously reported, SMOC2 plays a significant role in liver, kidney, and lung fibrosis [12, 32, 33]. However, studies on the role of SMOC2 in myocardial fibrosis are limited. Only one study has reported that SMOC2 alleviates myocardial fibrosis through the ILK/p38 pathway [15]. Our study also confirmed that SMOC2 was upregulated in myocardial fibrosis post-MI and in CFs treated under hypoxic conditions and that knockdown of SMOC2 could regulate the proliferation and differentiation of CFs. However, no studies have revealed the upstream regulatory mechanisms of SMOC2 in the proliferation and differentiation of CFs. Our study is the first to show that METTL3 affects the degradation rate of SMOC2 mRNA by modulating SMOC2 mRNA m6A methylation levels, thereby regulating SMOC2 expression. However, our study has several limitations. Firstly, owing to the difficulty in collecting human left ventricular samples, our research performed analysis with online public database. Secondly, while in this study we verified SMOC2 can affect the proliferation and differentiation of CFs, but its potential mechanism is not clear. Therefore, further research is necessary to unravel the downstream mechanism of SMOC2 in the proliferation and differentiation of CFs.

Conclusions

In summary, our research results indicate that METTL3 expression is increased in cardiac fibrosis post MI.We propose that METTL3 promotes the stability of SMOC2 mRNA by increasing the level of m6A methylation, thereby participating in CFs proliferation and differentiation after MI (Fig. 5). And our results are expected to provide new targets for the treatment of cardiac fibrosis.

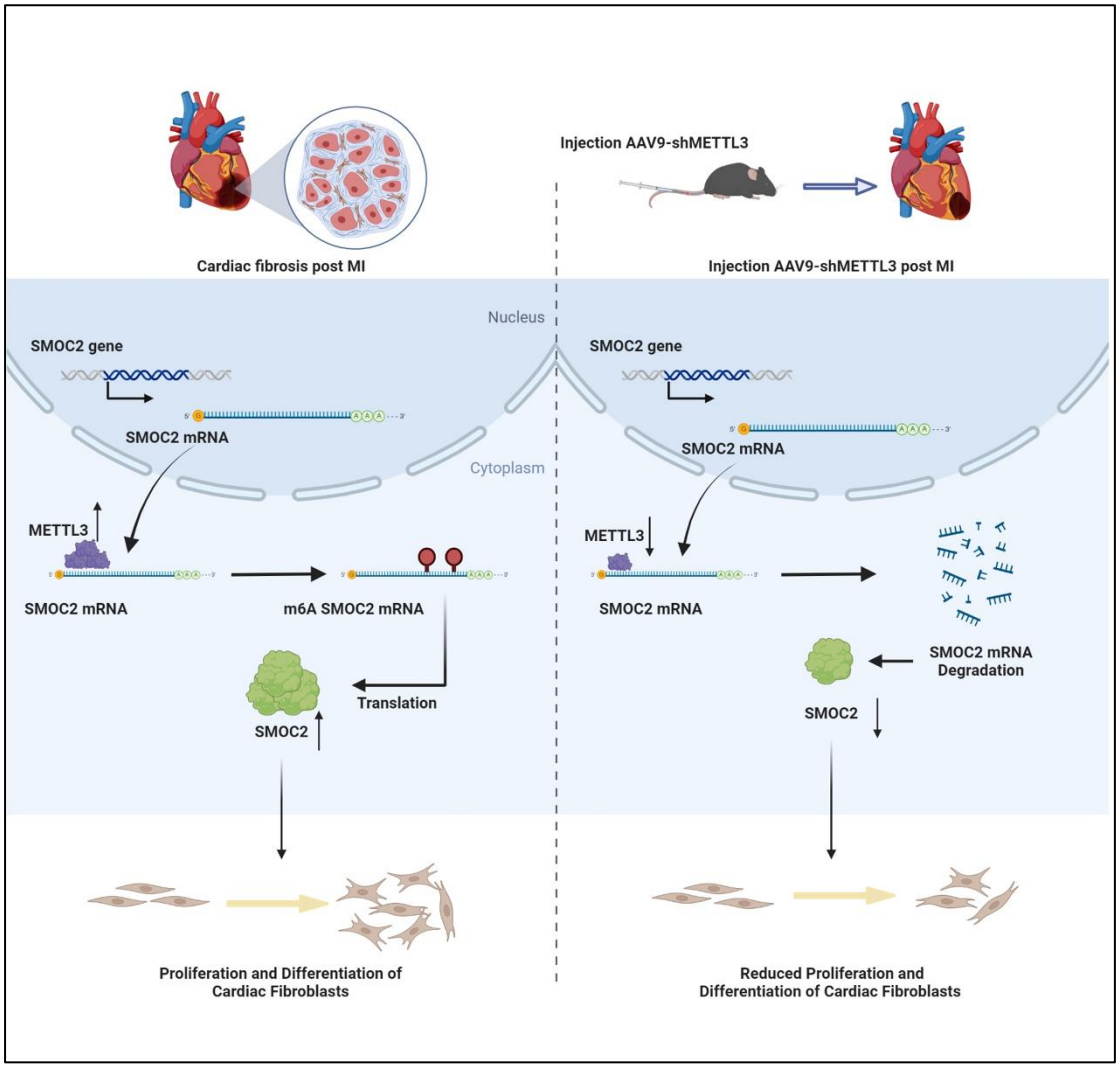

Fig. 5: The mechanistic scheme. A) METTL3 is increased post MI, and METTL3 promotes the stability of SMOC2 mRNA by increasing the level of m6A methylation, thereby participating in CFs proliferation and differentiation. B) Downregulation of

METTL3 leads to a decrease in the stability of SMOC2 mRNA by decreasing the level of m6A methylation, subsequently curtailing the proliferation and differentiation of CFs.

Author contributions:

YR H provided funding and wrote the manuscript. SK L and ZX T were responsible for the experiments and designed the study with GS Ma. XD P and ZP C provided vital reagents and analytical tools. Y L analyzed the data.

Funding

This work was supported by the National Natural Science Foundation of China (Grant Numbers 82000382).

Data availability statement

All data, models or code generated or used during the study are available from the corresponding author by request.

Declarations of competing interest: None.

Acknowledgements:

We thank all present and past members for their technical support. We would like to express our sincere gratitude to Editage for their professional editing and proofreading service. Additionally, we are deeply appreciative of BioRender for providing an

exceptional platform for creating high-quality scientific illustrations.

References

1. Virani SS, Alonso A, Benjamin EJ, Bittencourt MS, Callaway CW, Carson AP, Chamberlain AM, Chang AR, Cheng S, Delling FN, Djousse L, Elkind M, Ferguson JF, Fornage M, Khan SS, Kissela BM, Knutson KL, Kwan TW, Lackland DT, Lewis TT, Lichtman JH, Longenecker CT, Loop MS, Lutsey PL, Martin SS, Matsushita K, Moran AE, Mussolino ME, Perak AM, Rosamond WD, Roth GA, Sampson U, Satou GM, Schroeder EB, Shah SH, Shay CM, Spartano NL, Stokes A, Tirschwell DL, VanWagner LB, Tsao CW. Heart disease and stroke statistics-2020 update: a report from the american heart association. *Circulation* (2020) 141(9): e139-596. doi: 10.1161/CIR.0000000000000757.
2. Savarese G, Becher PM, Lund LH, Seferovic P, Rosano G, Coats A. Global burden of heart failure: a comprehensive and updated review of epidemiology. *Cardiovasc Res* (2023) 118(17):3272-87. doi: 10.1093/cvr/cvac013.
3. Roger VL. Epidemiology of heart failure: a contemporary perspective. *Circ Res* (2021) 128(10):1421-34. doi: 10.1161/CIRCRESAHA.121.318172.
4. He Y, Ling S, Sun Y, Sheng Z, Chen Z, Pan X, Ma G. Dna methylation regulates alpha-smooth muscle actin expression during cardiac fibroblast differentiation. *J Cell Physiol* (2019) 234(5):7174-85. doi: 10.1002/jcp.27471.
5. Pan X, Chen Z, Huang R, Yao Y, Ma G. Transforming growth factor beta1 induces the expression of collagen type i by dna methylation in cardiac fibroblasts. *Plos*

One (2013) 8(4):e60335. doi: 10.1371/journal.pone.0060335.

6. Meng Y, Xi T, Fan J, Yang Q, Ouyang J, Yang J. The inhibition of fto attenuates the antifibrotic effect of leonurine in rat cardiac fibroblasts. *Biochem Biophys Res Commun* (2024) 693:149375. doi: 10.1016/j.bbrc.2023.149375.
7. Tu B, Song K, Zhou Y, Sun H, Liu ZY, Lin LC, Ding JF, Sha JM, Shi Y, Yang JJ, Li R, Zhang Y, Zhao JY, Tao H. Mettl3 boosts mitochondrial fission and induces cardiac fibrosis by enhancing lncrna gas5 methylation. *Pharmacol Res* (2023) 194:106840. doi: 10.1016/j.phrs.2023.106840.
8. Li T, Zhuang Y, Yang W, Xie Y, Shang W, Su S, Dong X, Wu J, Jiang W, Zhou Y, Li Y, Zhou X, Zhang M, Lu Y, Pan Z. Silencing of mettl3 attenuates cardiac fibrosis induced by myocardial infarction via inhibiting the activation of cardiac fibroblasts. *Faseb J* (2021) 35(2):e21162. doi: 10.1096/fj.201903169R.
9. Zhou Y, Song K, Tu B, Sun H, Ding JF, Luo Y, Sha JM, Li R, Zhang Y, Zhao JY, Tao H. Mettl3 boosts glycolysis and cardiac fibroblast proliferation by increasing ar methylation. *Int J Biol Macromol* (2022) 223(Pt A):899-915. doi: 10.1016/j.ijbiomac.2022.11.042.
10. Yuting Y, Lifeng F, Qiwei H. Secreted modular calcium-binding protein 2 promotes high fat diet (hfd)-induced hepatic steatosis through enhancing lipid deposition, fibrosis and inflammation via targeting tgf-beta1. *Biochem Biophys Res Commun* (2019) 509(1):48-55. doi: 10.1016/j.bbrc.2018.12.006.
11. Gao Q, Mok HP, Zhuang J. Secreted modular calcium-binding proteins in pathophysiological processes and embryonic development. *Chin Med J (Engl)*

(2019) 132(20):2476-84. doi: 10.1097/CM9.0000000000000472.

12. Larsen FT, Hansen D, Terkelsen MK, Bendixen SM, Avolio F, Wernberg CW, Lauridsen MM, Gronkjaer LL, Jacobsen BG, Klinggaard EG, Mandrup S, Di Caterino T, Siersbaek MS, Indira CV, Graversen JH, Krag A, Grontved L, Ravnskjaer K. Stellate cell expression of sparc-related modular calcium-binding protein 2 is associated with human non-alcoholic fatty liver disease severity. *Jhep Rep* (2023) 5(2):100615. doi: 10.1016/j.jhepr.2022.100615.
13. Wang Y, Yang H, Su X, Cao A, Chen F, Chen P, Yan F, Hu H. Tgf-beta1/smoc2/akt and erk axis regulates proliferation, migration, and fibroblast to myofibroblast transformation in lung fibroblast, contributing with the asthma progression. *Hereditas* (2021) 158(1):47. doi: 10.1186/s41065-021-00213-w.
14. Schmidt IM, Colona MR, Kestenbaum BR, Alexopoulos LG, Palsson R, Srivastava A, Liu J, Stillman IE, Rennke HG, Vaidya VS, Wu H, Humphreys BD, Waikar SS. Cadherin-11, sparc-related modular calcium binding protein-2, and pigment epithelium-derived factor are promising non-invasive biomarkers of kidney fibrosis. *Kidney Int* (2021) 100(3):672-83. doi: 10.1016/j.kint.2021.04.037.
15. Rui H, Zhao F, Yuhua L, Hong J. Suppression of smoc2 alleviates myocardial fibrosis via the ilk/p38 pathway. *Front Cardiovasc Med* (2022) 9:951704. doi: 10.3389/fcvm.2022.951704.
16. Li D, Lin H, Li L. Multiple feature selection strategies identified novel cardiac gene expression signature for heart failure. *Front Physiol* (2020) 11:604241. doi: 10.3389/fphys.2020.604241.

17. Tu D, Xu Q, Zuo X, Ma C. Uncovering hub genes and immunological characteristics for heart failure utilizing rra, wgcna and machine learning. *Int J Cardiol Heart Vasc* (2024) 51:101335. doi: 10.1016/j.ijcha.2024.101335.
18. Su SA, Yang D, Wu Y, Xie Y, Zhu W, Cai Z, Shen J, Fu Z, Wang Y, Jia L, Wang Y, Wang JA, Xiang M. Ephrinb2 regulates cardiac fibrosis through modulating the interaction of stat3 and tgf-beta/smad3 signaling. *Circ Res* (2017) 121(6):617-27. doi: 10.1161/CIRCRESAHA.117.311045.
19. Wu S, Zhang S, Wu X, Zhou X. M(6)a rna methylation in cardiovascular diseases. *Mol Ther* (2020) 28(10):2111-19. doi: 10.1016/j.ymthe.2020.08.010.
20. Kumari R, Ranjan P, Suleiman ZG, Goswami SK, Li J, Prasad R, Verma SK. Mrna modifications in cardiovascular biology and disease: with a focus on m6a modification. *Cardiovasc Res* (2022) 118(7):1680-92. doi: 10.1093/cvr/cvab160.
21. Ravassa S, Lopez B, Treibel TA, San JG, Losada-Fuentenebro B, Tapia L, Bayes-Genis A, Diez J, Gonzalez A. Cardiac fibrosis in heart failure: focus on non-invasive diagnosis and emerging therapeutic strategies. *Mol Aspects Med* (2023) 93:101194. doi: 10.1016/j.mam.2023.101194.
22. Gonzalez A, Schelbert EB, Diez J, Butler J. Myocardial interstitial fibrosis in heart failure: biological and translational perspectives. *J Am Coll Cardiol* (2018) 71(15):1696-706. doi: 10.1016/j.jacc.2018.02.021.
23. Frantz S, Hundertmark MJ, Schulz-Menger J, Bengel FM, Bauersachs J. Left ventricular remodelling post-myocardial infarction: pathophysiology, imaging, and novel therapies. *Eur Heart J* (2022) 43(27):2549-61. doi:

10.1093/eurheartj/ehac223.

24. Bolivar S, Perez-Cantillo M, Monterroza-Torres J, Vasquez-Trincado C, Castellar-Lopez J, Mendoza-Torres E. The role of mettl3 in the progression of cardiac fibrosis. *Curr Top Med Chem* (2023) 23(26):2427-35. doi: 10.2174/1568026623666230825144949.
25. Xue T, Qiu X, Liu H, Gan C, Tan Z, Xie Y, Wang Y, Ye T. Epigenetic regulation in fibrosis progress. *Pharmacol Res* (2021) 173:105910. doi: 10.1016/j.phrs.2021.105910.
26. Li X, Yang Y, Chen S, Zhou J, Li J, Cheng Y. Epigenetics-based therapeutics for myocardial fibrosis. *Life Sci* (2021) 271:119186. doi: 10.1016/j.lfs.2021.119186.
27. Jiang X, Liu B, Nie Z, Duan L, Xiong Q, Jin Z, Yang C, Chen Y. The role of m6a modification in the biological functions and diseases. *Signal Transduct Target Ther* (2021) 6(1):74. doi: 10.1038/s41392-020-00450-x.
28. Qin Y, Li L, Luo E, Hou J, Yan G, Wang D, Qiao Y, Tang C. Role of m6a rna methylation in cardiovascular disease (review). *Int J Mol Med* (2020) 46(6):1958-72. doi: 10.3892/ijmm.2020.4746.
29. Zhuang Y, Li T, Hu X, Xie Y, Pei X, Wang C, Li Y, Liu J, Tian Z, Zhang X, Peng L, Meng B, Wu H, Yuan W, Pan Z, Lu Y. Metbil as a novel molecular regulator in ischemia-induced cardiac fibrosis via mettl3-mediated m6a modification. *Faseb J* (2023) 37(3):e22797. doi: 10.1096/fj.202201734R.
30. Song K, Sun H, Tu B, Zhou Y, Lin LC, Liu ZY, Li R, Yang JJ, Zhang Y, Zhao JY, Tao H. Wtap boosts lipid oxidation and induces diabetic cardiac fibrosis by enhancing ar

methylation. *Iscience* (2023) 26(10):107931. doi: 10.1016/j.isci.2023.107931.

31. Ding JF, Sun H, Song K, Zhou Y, Tu B, Shi KH, Lu D, Xu SS, Tao H. Igfbp3 epigenetic promotion induced by mettl3 boosts cardiac fibroblast activation and fibrosis. *Eur J Pharmacol* (2023) 942:175494. doi: 10.1016/j.ejphar.2023.175494.
32. Gerarduzzi C, Kumar RK, Trivedi P, Ajay AK, Iyer A, Boswell S, Hutchinson JN, Waikar SS, Vaidya VS. Silencing smoc2 ameliorates kidney fibrosis by inhibiting fibroblast to myofibroblast transformation. *Jci Insight* (2017) 2(8). doi: 10.1172/jci.insight.90299.
33. Luo L, Wang CC, Song XP, Wang HM, Zhou H, Sun Y, Wang XK, Hou S, Pei FY. Suppression of smoc2 reduces bleomycin (blm)-induced pulmonary fibrosis by inhibition of tgf-beta1/smads pathway. *Biomed Pharmacother* (2018) 105:841-47. doi: 10.1016/j.biopha.2018.03.058.